Quantum Chemical Modeling of Enzymatic Reactions: The Case of Decarboxylation

Rong-Zhen Liao,[†,‡] Jian-Guo Yu,[‡] and Fahmi Himo*,[†]

[†]Department of Organic Chemistry, Arrhenius Laboratory, Stockholm University, SE-10691 Stockholm, Sweden

[‡]College of Chemistry, Beijing Normal University, Beijing, 100875, People's Republic of China

S *Supporting Information*

ABSTRACT: We present a systematic study of the decarboxylation step of the enzyme aspartate decarboxylase with the purpose of assessing the quantum chemical cluster approach for modeling this important class of decarboxylase enzymes. Active site models ranging in size from 27 to 220 atoms are designed, and the barrier and reaction energy of this step are evaluated. To model the enzyme surrounding, homogeneous polarizable medium techniques are used with several dielectric constants. The main conclusion is that when the active site model reaches a certain size, the solvation effects from the surroundings saturate. Similar results have previously been obtained from systematic studies of other classes of enzymes, suggesting that they are of a quite general nature.

I. INTRODUCTION

The use of quantum chemical models of enzyme active sites has proven very powerful in the study of both enzyme reaction mechanisms and various active site properties.[1] The philosophy of the approach, commonly called the cluster approach, is to cut out a rather limited part of the enzyme active site, a cluster, and use accurate electronic structure methods to calculate geometries, energies, and other properties. The electronic structure method of choice has been density functional theory (DFT), in particular, the B3LYP hybrid functional.[2]

In the cluster approach, two procedures are commonly used to compensate for the fact that a large part of the enzyme is not treated explicitly. To account for possible steric effects exerted by the enzyme surroundings on the cluster, a number of centers, typically where truncations are made, are kept fixed in the geometry optimizations. This procedure is necessary to prevent unrealistic movements of the various groups of the active site.

To account for electrostatic polarization effects, dielectric cavity techniques are usually used. The surrounding enzyme is assumed to be a homogeneous polarizable continuum with some dielectric constant ε. The choice of this dielectric constant is somewhat arbitrary and has been a matter of discussion, but usually $\varepsilon = 4$ is used.

The combination of these two approximations has been shown to be a quite robust protocol that indeed is sufficient to elucidate reaction mechanisms, distinguish between different mechanistic scenarios, and analyze the roles of various parts in the active site. Ten years ago, typical cluster models consisted of ca. 50 atoms, while today 150 atom models are quite common. Consequently, the scope of applications has been broadened considerably. Through the large number of applications in recent years, it has been demonstrated that the approach has a wide applicability, as essentially all classes of enzymes have been modeled quite successfully.[3]

It is easy to realize that as the size of the model grows, a better description of the active site is achieved, and both the

**Scheme 1. Reaction Catalyzed by AspDC**
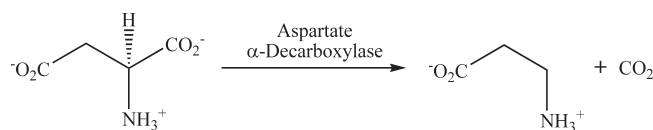
coordinate-locking scheme and the implicit solvation model will work better and better because the model will be more flexible and more of the polarization effects will be already explicitly included in the cluster model. The question has been how large a model one needs to use before the effects saturate. Saturation of solvation effects in this sense means that the addition of these does not influence the energy profile of the reaction under investigation; i.e., the relative energies are the same with and without the inclusion of implicit solvation. At that point, the exact choice of the dielectric constant becomes an irrelevant issue.

Recently, by performing systematic studies in which the size of the cluster model was gradually increased, we have shown that saturation of the solvation effect happens surprisingly fast, at a model size of less than 200 atoms. This has been demonstrated for three cases that potentially could be problematic for the cluster approach, namely, (a) the formation of an ion pair in the reaction of 4-oxalocrotonate tautomerase (4-OT),[4] (b) the release of a chloride ion in the reaction of haloalcohol dehalogenase (HheC),[5] and (c) the transfer of a methyl cation in the reaction of histone lysine methyltransferase (HKMT).[6]

In the present paper, we further examine the scope of this cluster methodology by studying another important class of enzymes, namely, decarboxylases. Here, from being an anionic moiety (R—COO), CO_2 is released as a neutral gas, which could provide additional challenges where the cluster approach needs to be evaluated.

Scheme 2. Suggested Reaction Mechanism of AspDC^a
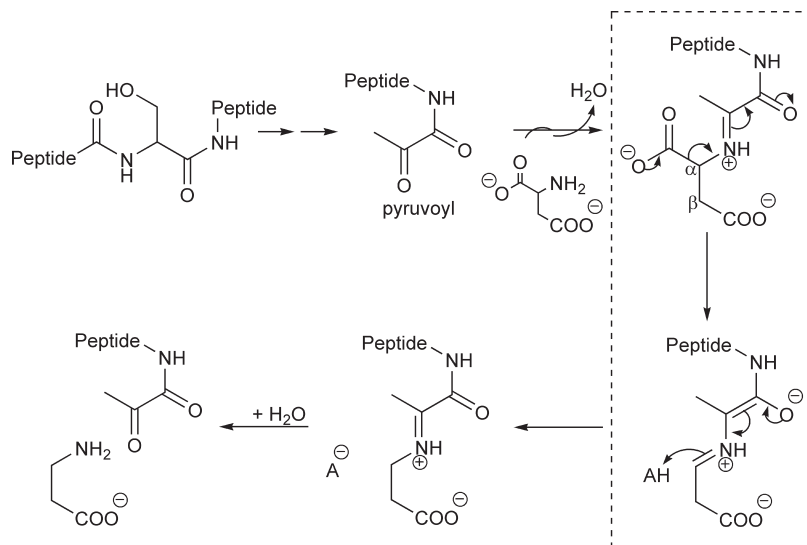
^{a} The frame indicates the C—C cleavage step studied in the present work.
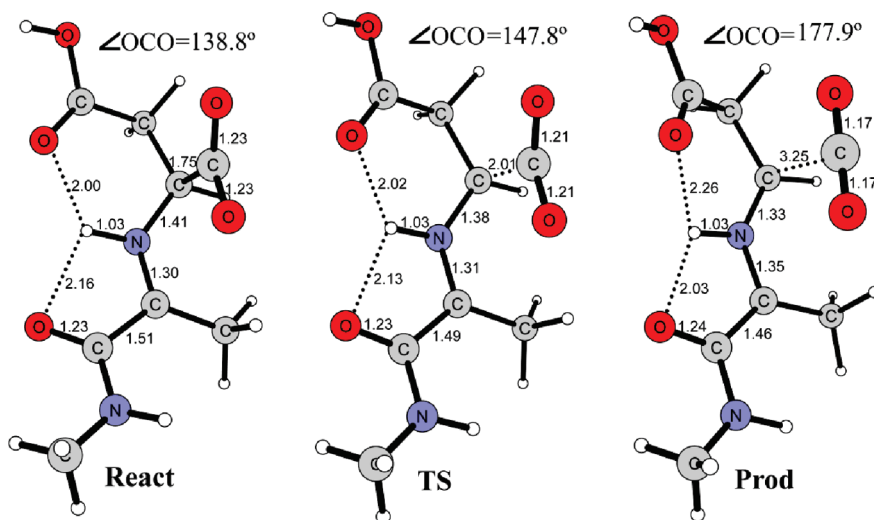
Figure 1. Optimized structures of the reactant, transition state, and product for model 0. Distances in Ångstroms. The carboxylate $\angle$OCO angle is indicated.

A number of enzymes catalyzing carboxylation/decarboxylation reactions have previously been studied both with the cluster approach[7] and with QM/MM methodologies.[8] The specific enzyme considered in the present work is L-aspartate α-decarboxylase (AspDC), which catalyzes the decarboxylation of L-aspartate to β-alanine (Scheme 1).[9] This reaction is essential for the biosynthesis of pantothenate (vitamin B5) and coenzyme A in bacteria.[10]

AspDC belongs to the class of decarboxylases that utilize a covalently bound pyruvoyl group that is generated through an autoproteolytic cleavage reaction.[9c,11] The suggested reaction mechanism for AspDC is given in Scheme 2.[12] It involves an initial iminium formation step, followed by a C—C bond cleavage step which releases the carbon dioxide. Protonation and hydrolysis steps complete the reaction to give the final product and regenerate the pyruvoyl cofactor.

Because we are, in the present paper, only interested in the methodological issues, we will assume that this mechanism is correct and will focus only on the key C—C cleavage step. Several models of the AspDC active site are systematically devised to investigate how the reaction energetics and solvation effects change with the model size.

II. COMPUTATIONAL DETAILS

All calculations presented herein were performed using the density functional theory method B3LYP as implemented in Gaussian 03.[13] For geometry optimizations, the 6-31G(d,p) basis set was used. In order to obtain more accurate energies, single-point calculations based on the optimized geometries were done using the 6-311+G$(2d,2p)$ basis set. Solvation effects were calculated at the same level as the geometry optimizations by

1495

dx.doi.org/10.1021/ct200031t |*J. Chem. Theory Comput.* 2011, 7, 1494–1501

performing single-point calculations on the optimized structures using the conductor-like polarizable continuum model method (CPCM).[14] Five different dielectric constants were used, namely $\varepsilon = 2, 4, 8, 16,$ and 80. For models 0, I, II, and III (see below), zero-point energy (ZPE) corrections were calculated at the same level as geometry optimizations. For models IV.1, IV.2, and V, the size of the models prohibited the frequency calculations. Thus, for these models, the ZPE correction was taken from model III.

As discussed in the Introduction, a number of atoms are kept fixed during the geometry optimizations to prevent unrealistic movements of the various groups in the models. This technique leads to a few small imaginary frequencies, in this case all below $40i$ cm^{-1}. These frequencies contribute insignificantly to the ZPE and can be ignored. However, they make the calculation of harmonic entropy effects inaccurate. Therefore, the entropy effects were not considered for models I–V, see discussion below.

It is important to point out here that when working with large models of enzyme active sites, like the ones used in the present work, multiple-minima problems can appear, which can lead to unreliable relative energies. We have, by careful visual inspection, confirmed that the parts that do not directly participate in the reaction are in the same local minima throughout the reaction.

Table 1. Summary of the Calculated Energetics (kcal/mol) for the Decarboxylation Step Using Various Models of AspDC

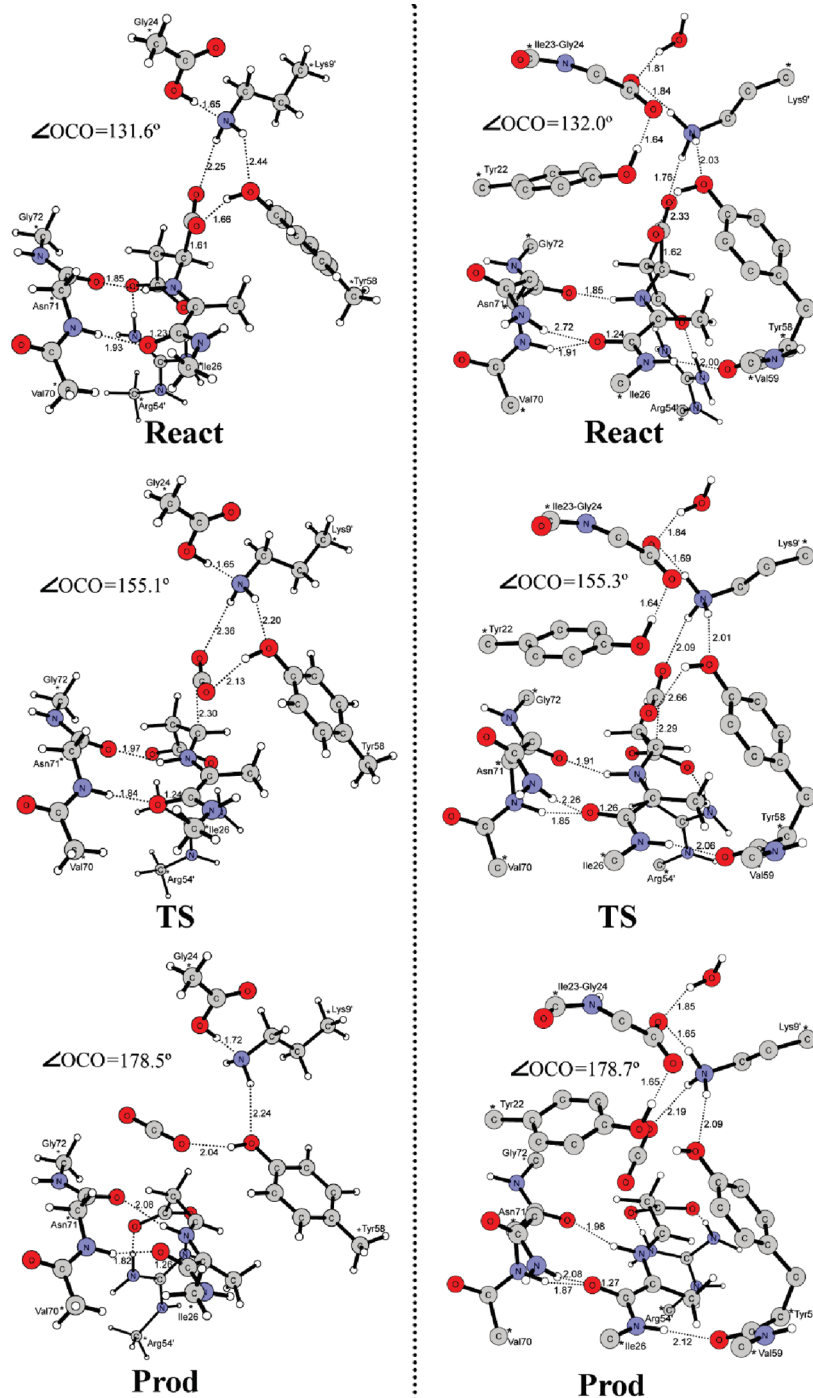|		$\varepsilon = 1$	$\varepsilon = 2$	$\varepsilon = 4$	$\varepsilon = 8$	$\varepsilon = 16$	$\varepsilon = 80$
model 0 (27 atoms)	$\Delta E^{\ddagger}$	0.1	2.3	3.7	4.5	4.9	5.2
	ΔE	−9.5	−5.7	−3.5	−2.2	−1.5	−1.0
model I (76 atoms)	$\Delta E^{\ddagger}$	8.3	12.0	14.2	15.5	16.1	16.7
	ΔE	+0.3	+2.9	+4.5	+5.5	+6.0	+6.5
model II (95 atoms)	$\Delta E^{\ddagger}$	8.8	11.9	13.6	14.7	15.3	15.7
	ΔE	−0.6	+2.6	+4.5	+5.6	+6.2	+6.7
model III (135 atoms)	$\Delta E^{\ddagger}$	9.0	11.4	12.9	13.5	13.9	14.2
	ΔE	+0.8	+2.5	+3.5	+4.1	+4.3	+4.6
model IV.1 (166 atoms)	$\Delta E^{\ddagger}$	13.9	13.1	12.7	12.5	12.4	12.3
	ΔE	+9.9	+8.7	+8.0	+7.6	+7.4	+7.2
model IV.2 (189 atoms)	$\Delta E^{\ddagger}$	13.0	15.6	17.0	17.8	18.2	18.5
	ΔE	+4.2	+7.7	+9.8	+9.9	+10.5	+10.9
model V (220 atoms)	$\Delta E^{\ddagger}$	13.5	13.5	13.4	13.3	13.3	13.3
	ΔE	+9.0	+9.6	+9.9	+10.0	+10.0	+10.0
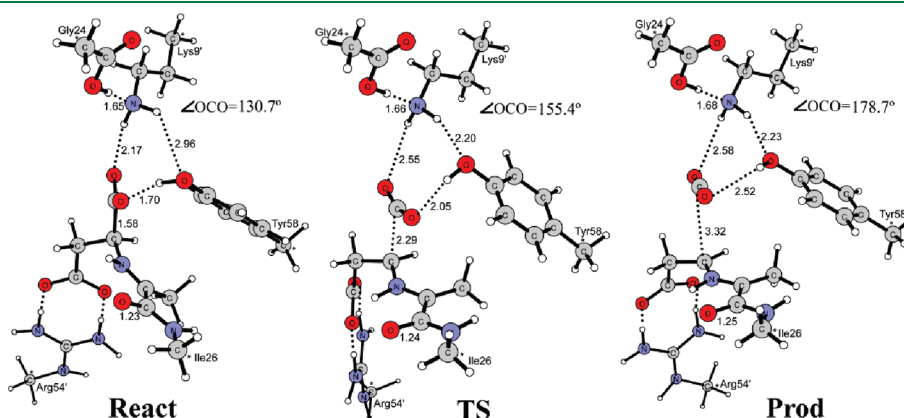
The above-mentioned coordinate locking scheme facilitates this procedure to some extent.

III. RESULTS AND DISCUSSION

III.A. Pyruvoyl-Catalyzed Decarboxylation. We first consider the decarboxylation step of only the substrate covalently bound to the pyruvoyl, i.e., without any surrounding active site residues. In this model, which we call model 0, the cofactor is truncated at the α-carbon of Ile26 and the β-carboxylic group of the substrate aspartate is in the protonated form. In the active site, this group forms salt bridges to the Arg54′ residue, and when the latter is not explicitly included in the model, it is a better choice to protonate the group rather than using the anion model to avoid charge delocalization problems in the calculations.[15] The model consists of 27 atoms and has a total charge of 0. The optimized structures of the reactant, transition state (TS), and product species are shown in Figure 1.

In the catalytic cycle of AspDC, the formation of the Schiff base (iminium intermediate) leads to weakening of the C–C bond and hence the facilitation of the decarboxylation step. In the zwitterionic reactant structure of model 0, we see that the positive charge at NH is stabilized by two hydrogen bonds to the neighboring β-carboxylic acid group and the carbonyl oxygen. It is interesting to note how the scissile C–C bond is weakened, having a bond length of 1.75 Å, considerably longer than a normal C–C single bond length. Indeed, the barrier for decarboxylation is calculated to be very low for this model. In the gas phase, the step is practically barrierless (+0.1 kcal/mol) with an exothermicity of 9.5 kcal/mol. The addition of solvation effects, however, increases both the barrier and the reaction energy, because the zwitterionic reactant structure is stabilized more than the TS and product structures. The barrier increases to, e.g., 5.2 kcal/mol, and the reaction energy becomes only −1.0 kcal/mol when $\varepsilon = 80$ is used. All energies are reported in Table 1.

Before presenting the results concerning the active site models, one additional issue needs to be discussed here, namely, the entropic effects. The decarboxylation step results in the decomposition of the reactant molecule into two, an imine and a carbon dioxide. The entropy effects could potentially contribute in a non-negligible way to the energetics. We have calculated the harmonic entropy effects for model 0, and it turns out that at room temperature (298.15 K), the entropy effects increase the

Figure 2. Optimized stationary points for model I. Centers indicated by asterisks are kept fixed during the geometry optimizations.

Figure 3. Optimized structures of the reactant, transition state, and product for model II (left) and model III (right). In this and the following figures, some hydrogen atoms are removed for clarity.

barrier by less than 0.1 kcal/mol. This is a very important result that justifies the omission of entropy effects for the barriers in the active site models. It is also consistent with results from QM/MM free energy calculations on the histone lysine methyltransferase enzyme, where it was found that the potential energy and the free energy barriers differed by only 1 kcal/mol.[16] Very similar conclusions were reached by Thiel and co-workers in their studies on p-hydroxybenzoate hydroxylase, 5′-fluoro-5′-deoxyadenosine synthase, P450cam, and chorismate mutase.[17]

For the products complex, on the other hand, the entropy effects become larger of course, since CO_2 has completely dissociated from the molecule. This leads to a lowering of the reaction energy by 4.2 kcal/mol.

III.B. Active Site Model I. In the following sections, we discuss how the inclusion of active site surrounding groups affects the energetics of this reaction. Six models, gradually increased from 76 to 220 atoms, were constructed on the basis of the high-resolution crystal structure of AspDC
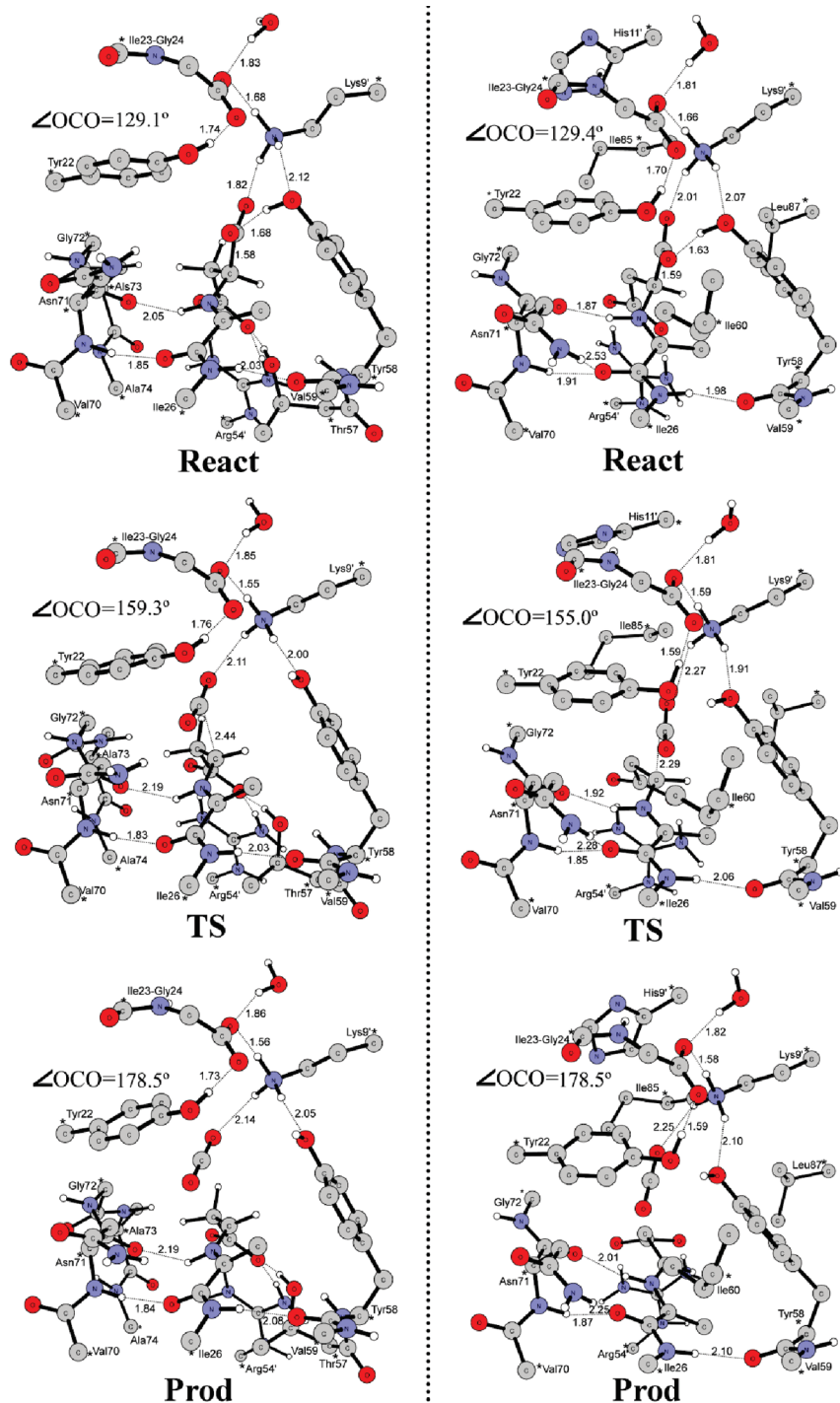
Figure 4. Optimized structures for models IV.1 and IV.2.

from *H. pylori* in complex with aspartate amide (PDB code: 1UHE).[18]

The first obvious places to add groups to model 0 are the two carboxylate groups of the substrate. To the α-carboxylate group that is going to be cleaved, two hydrogen bond donors were added, Tyr58 (modeled by a methylphenol) and Lys9′ (modeled by propylamine). In addition, the carboxylic moiety of the Gly24 (generated in the autocleavage step), which forms a hydrogen

bond to Lys9′, is also included (modeled by an acetate molecule), as it will affect the hydrogen-bonding properties of the lysine. The β-carboxylate, which in model 0 was in the protonated from, is now in the ionized form but forming salt bridges to the cationic Arg54′ residue (modeled by a methyl-guanidinium). The resulting model, called model I and shown in Figure 2, consists thus of 76 atoms and has a total charge of 0.
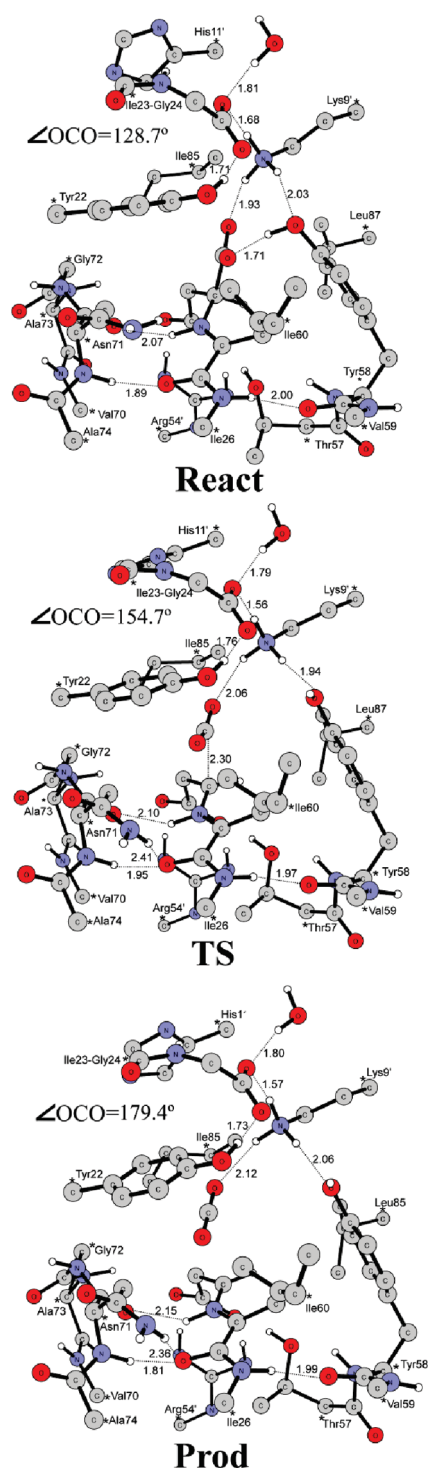
Figure 5. Optimized structures for model V.

Without solvation, the calculated barrier now is 8.3 kcal/mol and the reaction energy is +0.3 kcal/mol (Table 1). These values are 8–10 kcal/mol higher than the corresponding ones for model 0. This is mainly because the added hydrogen bonds provided by Lys9′ and Tyr58 are stronger to the anionic moiety of the reactant as compared to the TS and neutral carbon dioxide in the product, see Figure 2.

Upon inclusion of solvation effects, both the barrier and the reaction energy increase further (see Table 1). With $\varepsilon = 4$

and $\varepsilon = 80$, for example, the barrier increases to 14.2 and 16.7 kcal/mol, respectively, and the reaction energy increases to +4.5 and +6.5 kcal/mol, respectively. The solvation effects are quite large, and additional groups are clearly needed.

III.C. Active Site Model II. Next, on the basis of model I, the peptide backbone chain between Val70, Asn71, and Gly72 was added (Figure 3). These groups form hydrogen bonds to the iminium NH and the amide carbonyl. With this addition, the active site model (model II) now consists of 95 atoms.

As seen from Figure 3, the critical geometric parameters in the transition state are quite similar to those obtained from model I, with a C–C distance of 2.30 Å and an $\angle$ OCO angle of 155.1°. The calculated barrier for model II is 8.8 kcal/mol, and the reaction energy is −0.6 kcal/mol. Both of these values are also quite close to the ones calculated for model I. The solvation effects are still large. For example, both the barrier and the reaction energy increase by ca. 5 and 7 kcal/mol using $\varepsilon = 4$ and $\varepsilon = 80$, respectively.

We see thus that although two explicit hydrogen bonds to the substrate are added to the model, the energies and solvation effects are not changed significantly compared to model I, indicating that more groups need to be included in the active site model.

III.D. Active Site Model III. On the basis of model II, a larger model consisting of 135 atoms was designed, called model III, see Figure 3. In this model, the Gly24 residue is extended to include the peptide bond to Ile23 to give the group more flexibility. Tyr22 and a crystallographically observed water molecule are included to stabilize the negative charge of Gly24 carboxylate. Furthermore, the Val59-Tyr58 peptide and the side chain of Asn71, which form two hydrogen bonds to the Ile26-pyruvoyl amide group, are also included.

Because of the newly added groups around the carboxylic moiety of Gly24, this group is now in the deprotonated anionic form (R–COO⁻), and the Lys9′ side chain is in the protonated cationic form (R–NH₃⁺) in the reactant complex of model III. The hydrogen bond (1.76 Å) between Lys9′ and the substrate carboxylate group becomes stronger compared to that in model II (2.25 Å). It is interesting to note that in the transition state, the key C–C distance is 2.29 Å and the $\angle$ OCO is 155.2°, which are very close to those in model II. The barrier is 9.0 kcal/mol, and the product lies at +0.8 kcal/mol, also quite close to the values found for model II. The solvation effects are now somewhat smaller. For instance, the barrier increases to 12.9 and 14.2 kcal/mol, and the reaction energy increases to +3.5 and +4.6 kcal/mol using $\varepsilon = 4$ and $\varepsilon = 80$, respectively.

Although the solvation effects are now smaller than before, they are still of considerable size, and clearly more groups need to be added before saturation is reached.

III.E. Active Site Model IV. Model III was increased in two different ways, and the resulting models are called models IV.1 and IV.2 and consist of 166 and 189 atoms, respectively. They differ in where the addition is made. In model IV.1, the region around the substrate β-carboxylate and the iminium part of the substrate is extended by Thr57 and the Gly72-Ala73-Ala74 peptide chain, while in model IV.2, the region around the α-carboxylate is extended by the Ile60, Ile85, and Leu87 residues (see Figure 4).

The two extensions lead to significant and different changes in both the energies and the solvation effects as compared to model III.

In model IV.1, the barrier is calculated to be 13.9 kcal/mol, and the reaction energy is +9.9 kcal/mol. In contrast to all previous

1499

dx.doi.org/10.1021/ct200031t |*J. Chem. Theory Comput.* 2011, 7, 1494–1501

models, the solvation now causes a lowering of both the barrier and the reaction energy. The solvation effects are also getting smaller compared to the previous models (less than 2 kcal/mol for the barrier and less than 3 kcal/mol for the reaction energy).

Model IV.2, on the other hand, has a barrier of 13.0 kcal/mol and a reaction energy of 4.2 kcal/mol, both of which are raised by up to 5−7 kcal/mol upon the addition of solvation.

These different results for models IV.1 and IV.2 show thus that the newly added groups influence the model energies in different ways. The next obvious model is to combine these two.

III.F. Active Site Model V. In model V, all of the groups added in models IV.1 and IV.2 are combined into a 220 atom model, the largest one used in this study (Figure 5).

The barrier now is 13.5 kcal/mol, and the reaction energy is +9.0 kcal/mol. As seen from Table 1, the addition of solvation effects, even with the largest dielectric constant ($\varepsilon = 80$), leads to a change of the vanishingly small 0.2 kcal/mol for the barrier and 1.0 kcal/mol for the reaction energy. Most of the polarization effects on the reactive parts are thus already explicitly included in the cluster model, and the solvation effects can be considered as saturated at this size.

It is also very interesting to note that the optimized transition state for this model has a very similar local geometry to those of the other models discussed above. For example, the dissociating C−C bond distance is 2.30 Å and the ∠OCO angle is 154.7°.

IV. CONCLUSIONS

In the present study, we have investigated how the quantum chemical cluster approach works for the case of enzymatic decarboxylation reactions, as exemplified by aspartate decarboxylase (AspDC). The size of the active site model is systematically increased, and the reaction barrier and energy are evaluated using several dielectric constants for the homogeneous surrounding.

The calculations show that once the model reaches a certain size (in this case 220 atoms) the solvation effects saturate; i.e., the relative energies are essentially the same whether the homogeneous surrounding is included or not (see Table 1). We have observed this quick convergence for several examples of different classes of enzymes, namely, 4-oxalocrotonate tautomerase,[4] in which an ion pair is formed during the reaction; haloalcohol dehalogenase HheC,[5] in which a chloride ion is released; and histone lysine methyltransferase,[6] in which a methyl cation is transferred. Taken together, these results suggest thus that this is a general feature of the cluster approach.

Of course, as pointed out by Ryde and co-workers,[19] convergence of the solvation effects is not equivalent to convergence of the energies (barriers and reaction energies), although they might be related. In this context, it is particularly interesting to note that the energies of all active site models (I−V) after application of some solvation corrections fall within a relatively narrow range of about 5 kcal/mol. This shows that the results are quite stable and are already using medium-sized models certainly in a sufficiently accurate manner to investigate mechanistic alternatives. Considering this, it is also unlikely that groups that are further away will affect the relative energies in any significant way.

Here, it should be remembered that geometry optimization of the structures is an essential requirement of the cluster approach, contributing to the quick convergence observed. By contrast, the QM/MM methodology exhibits a quite slow convergence behavior,[19−21] which in part could be due to the fact that geometries are not optimized.[19,20]

■ ASSOCIATED CONTENT

ⓈSupporting Information. Cartesian coordinates for all structures. This material is available free of charge via the Internet at http://pubs.acs.org.

■ AUTHOR INFORMATION

Corresponding Author
*E-mail: himo@organ.su.se.

■ ACKNOWLEDGMENT

■ REFERENCES

(1) For reviews, see: (a) Blomberg, M. R. A.; Siegbahn, P. E. M. *J. Phys. Chem. B* **2001**, *105*, 9375–9386. (b) Himo, F.; Siegbahn, P. E. M. *Chem. Rev.* **2003**, *103*, 2421–2456. (c) Noodleman, L.; Lovell, T.; Han, W.-G.; Li, J.; Himo, F. *Chem. Rev.* **2004**, *104*, 459–508. (d) Siegbahn, P. E. M.; Borowski, T. *Acc. Chem. Res.* **2006**, *39*, 729–738. (e) Himo, F. *Theor. Chem. Acc.* **2006**, *116*, 232–240. (f) Ramos, M. J.; Fernandes, P. A. *Acc. Chem. Res.* **2008**, *41*, 689–698. (g) Himo, F.; Siegbahn, P. E. M. *J. Biol. Inorg. Chem.* **2009**, *14*, 643–651. (h) Blomberg, M. R. A.; Siegbahn, P. E. M. *Biochim. Biophys. Acta* **2010**, *1797*, 129–142.

(2) (a) Becke, A. D. *J. Chem. Phys.* **1993**, *98*, 5648–5652. (b) Lee, C.; Yang, W.; Parr, R. G. *Phys. Rev. B* **1988**, *37*, 785–789.

(3) See for example the following applications: (a) Velichkova, P.; Himo, F. *J. Phys. Chem. B* **2005**, *109*, 8216–8219. (b) Hopmann, K. H.; Himo, F. *Chem.—Eur. J.* **2006**, *12*, 6898–6909. (c) Hopmann, K. H.; Guo, J.-D.; Himo., F. *Inorg. Chem.* **2007**, *46*, 4850–4856. (d) De Marothy, S. A.; Blomberg, M. R. A.; Siegbahn, P. E. M. *J. Comput. Chem.* **2007**, *28*, 528–539. (e) Leopoldini, M.; Chiodo, S. G.; Toscano, M.; Russo, N. *Chem.—Eur. J.* **2008**, *14*, 8647–8681. (f) Borowski, T.; Blomberg, M. R. A.; Siegbahn, P. E. M. *Chem.—Eur. J.* **2008**, *14*, 2264–2276. (g) Sevastik, R.; Whitman, C. P.; Himo, F. *Biochemistry* **2009**, *48*, 9641–9649. (h) Chen, S.-L.; Pelmenschikov, V.; Blomberg, M. R. A.; Siegbahn, P. E. M. *J. Am. Chem. Soc.* **2009**, *131*, 9912–9913. (i) Sousa, S. F.; Fernandes, P. A.; Ramos, M. J. *Chem.—Eur. J.* **2009**, *15*, 4243–4247. (j) Roos, K.; Siegbahn, P. E. M. *Biochemistry* **2009**, *48*, 1878–1887. (k) Yang, L.; Liao, R.-Z.; Yu, J.-G.; Liu, R.-Z. *J. Phys. Chem. B* **2009**, *113*, 6505–6510. (l) Parks, J. M.; Guo, H.; Momany, C.; Liang, L. Y.; Miller, S. M.; Summers, A. O.; Smith, J. C. *J. Am. Chem. Soc.* **2009**, *131*, 13278–13285. (m) Liao, R.-Z.; Yu, J.-G.; Himo, F. *J. Phys. Chem. B* **2010**, *114*, 2533–2540.

(4) Sevastik, R.; Himo, F. *Bioorg. Chem.* **2007**, *35*, 444–457.

(5) Hopmann, K. H.; Himo, F. *J. Chem. Theory Comput.* **2008**, *4*, 1129–1137.

(6) Georgieva, P.; Himo, F. *J. Comput. Chem.* **2010**, *31*, 1707–1714.

(7) (a) Lee, J. K.; Houk, K. N. *Science* **1997**, *276*, 942–945. (b) Lundberg, M.; Blomberg, M. R. A.; Siegbahn, P. E. M. *J. Mol. Model* **2002**, *8*, 119–130. (c) Silva, P. J.; Ramos, M. J. *J. Phys. Chem. B* **2005**, *109*, 18195–18200. (d) Wang, J.; Hong, H.; Li, S.; He, H. *J. Phys. Chem. B* **2005**, *109*, 18664–18672. (e) Silva, P. J.; Ramos, M. J. *J. Phys. Chem. B* **2007**, *111*, 12883–12887. (f) Ito, Y.; Kondo, H.; Shiota, Y.; Yoshizawa, K. *J. Chem. Theory Comput.* **2008**, *4*, 366–374.

(8) (a) Wu, N.; Mo, Y.; Gao, J.; Pai, E. F. *Proc. Natl. Acad. Sci. U.S.A.* **2000**, *97*, 2017–2022. (b) Lee, T.-S.; Chong, L. T.; Chodera, J. D.; Kollman, P. A. *J. Am. Chem. Soc.* **2001**, *123*, 12837–12848. (c) Stanton, C. L.; Kuo, I. W.; Mundy, C. J.; Laino, T.; Houk, K. N. *J. Phys. Chem. B* **2007**, *111*, 12573–12581. (d) Moya-García, A. A.; Ruiz-Pernía, J.; Martí, S.; Sánchez-Jiménez, F.; Tuñón, I. *J. Biol. Chem.* **2008**, *283*, 12393–12401. (e) Hu, H.; Boone, A.; Yang, W. *J. Am. Chem. Soc.* **2008**, *130*, 14493–14503. (f) Lin, Y.-L.; Gao, J. L. *J. Am. Chem. Soc.* **2011** [Online] dx.doi.org/10.1021/ja108209w.

(9) (a) Williamson, J. M.; Brown, G. M. *J. Biol. Chem.* **1979**, *254* 8074–8082. (b) Cronan, J. E., Jr. *J. Bacteriol.* **1980**, *141*, 1291–1297. (c) van Poelje, P. D.; Snell, E. E. *Annu. Rev. Biochem.* **1990**, *59*, 29–59. (d) Ramjee, M. K.; Genschel, U.; Abell, C.; Smith, A. G. *Biochem. J.* **1997**, *323*, 661–669. (e) Chopra, S. C.; Pai, H.; Ranganathan, A. *Protein Expression Purif.* **2002**, *25*, 533–540.

(10) Brown, G. M.; Williamson, J. M. *Adv. Enzymol. Relat. Areas Mol. Biol.* **1982**, *53*, 345–381.

(11) (a) Recsei, P. A.; Huynh, Q. K.; Snell, E. E. *Proc. Natl. Acda. Sci. U.S.A.* **1983**, *80*, 973–977. (b) Albert, A.; Dhanaraj, V.; Genschel, U.; Khan, G.; Ramjee, M. K.; Pulido, R. *Nat. Struct. Biol.* **1998**, *5*, 289–293. (c) Xiong, H.; Pegg, A. E. *J. Biol. Chem.* **1999**, *274*, 35059–35066. (d) Schmitzberger, F.; Kilkenny, M. L.; Lobley, C. M. C.; Webb, M. E.; Vinkovic, M.; Matak-Vinkovic, D.; Witty, M.; Chirgadze, D. Y.; Smith, A. G.; Abell, C.; Blundell, T. L. *EMBO J.* **2003**, *22*, 6193–6204.

(12) Saldanha, S. A.; Birch, L. M.; Webb, M. E.; Nabbs, B. K.; von Delft, F.; Smith, A. G.; Abell, C. *Chem. Commun.* **2001**, 1760–1761.

(13) Frisch, M. J.; Trucks, G. W.; Schlegel, H. B.; Scuseria, G. E.; Robb, M. A.; Cheeseman, J. R.; Montgomery, J. A., Jr.; Vreven, T.; Kudin, K. N.; Burant, J. C.; Millam, J. M.; Iyengar, S. S.; Tomasi, J.; Barone, V.; Mennucci, B.; Cossi, M.; Scalmani, G.; Rega, N.; Petersson, G. A.; Nakatsuji, H.; Hada, M.; Ehara, M.; Toyota, K.; Fukuda, R.; Hasegawa, J.; Ishida, M.; Nakajima, T.; Honda, Y.; Kitao, O.; Nakai, H.; Klene, M.; Li, X.; Knox, J. E.; Hratchian, H. P.; Cross, J. B.; Bakken, V.; Adamo, C.; Jaramillo, J.; Gomperts, R.; Stratmann, R. E.; Yazyev, O.; Austin, A. J.; Cammi, R.; Pomelli, C.; Ochterski, J. W.; Ayala, P. Y.; Morokuma, K.; Voth, G. A.; Salvador, P.; Dannenberg, J. J.; Zakrzewski, V. G.; Dapprich, S.; Daniels, A. D.; Strain, M. C.; Farkas, O.; Malick, D. K.; Rabuck, A. D.; Raghavachari, K.; Foresman, J. B.; Ortiz, J. V.; Cui, Q.; Baboul, A. G.; Clifford, S.; Cioslowski, J.; Stefanov, B. B.; Liu, G.; Liashenko, A.; Piskorz, P.; Komaromi, I.; Martin, R. L.; Fox, D. J.; Keith, T.; Al-Laham, M. A.; Peng, C. Y.; Nanayakkara, A.; Challacombe, M.; Gill, P. M. W.; Johnson, B.; Chen, W.; Wong, M. W.; Gonzalez, C.; Pople, J. A. *Gaussian 03*, revision D.01; Gaussian, Inc.: Wallingford, CT, 2004.

(14) (a) Klamt, A.; Schüürmann, G. *J. Chem. Soc., Perkin. Trans.* **1993**, *2*, 799–805. (b) Andzelm, J.; Kölmel, C.; Klamt, A. *J. Chem. Phys.* **1995**, *103*, 9312–9320. (c) Barone, V.; Cossi, M. *J. Phys. Chem. A* **1998**, *102*, 1995–2001. (d) Cossi, M.; Rega, N.; Scalmani, G.; Barone, V. *J. Comput. Chem.* **2003**, *24*, 669–691.

(15) (a) Himo, F.; Eriksson, L. A. *J. Am. Chem. Soc.* **1998**, *120*, 11449–11455. (b) Guo, J.-D.; Himo, F. *J. Phys. Chem. B* **2004**, *108*, 15347–15354. (c) Condic-Jurikic, K.; Perchyonok, V. T.; Zipse, H.; Smith, D. M. *J. Comput. Chem.* **2008**, *29*, 2425–2433.

(16) Hu, P.; Zhang, Y. *J. Am. Chem. Soc.* **2006**, *128*, 1272–1278.

(17) (a) Senn, H. M.; Thiel, S; Breidung, J.; Thiel, W. *J. Chem. Theory Comput.* **2005**, *1*, 494–505. (b) Senn, H. M.; Kästner, J.; Breidung, J.; Thiel, W. *Can. J. Chem.* **2009**, *87*, 1332–1337.

(18) Lee, B. I.; Suh, S. W. *J. Mol. Biol.* **2004**, *340*, 1–7.

(19) Hu, L. H.; Eliasson, J.; Heimdal, J.; Ryde, U. *J. Phys. Chem. A* **2009**, *113*, 11793–11800.

(20) Sumowski, C. V.; Ochsenfeld, C. *J. Phys. Chem. A* **2009**, *113*, 11734–11741.

(21) Solt, I.; Kulhánek, P.; Simon, I.; Winfield, S.; Payne, M. C.; Csányi, G.; Fuxreiter, M. *J. Phys. Chem. B* **2009**, *113*, 5728–5735.